Design benefits for plate anchors for floating offshore wind through coupling floater, mooring and geotechnical responses

K.A. Kwa, O. Festa, D.J White, S. Gourvenec,
University of Southampton, Southampton, UK

A. Sobey
The Alan Turing Institute, British Library, UK
University of Southampton, Southampton, UK

ABSTRACT: This study presents analysis of a floating offshore wind system to illustrate methodologies for reducing the mooring loads transmitted to the anchor and the required anchor size. These design efficiencies support acceleration of the development of floating offshore wind, to help meet the growth required for 2050 net zero targets. The anchor loading and size reductions are achieved by combining techniques that i) reduce the anchor loads by considering load reduction devices (LRD) in the mooring line configuration, and ii) mobilise additional seabed resistance by considering beneficial seabed effects due to inertia and changing strength. This study demonstrates the benefits of combining these effects through an integrated floater-mooring and anchor-seabed analysis approach. The method is applied to an example whole-life application spanning the operating life of a floating offshore wind (FOW) system. This analysis indicates a potential 50% reduction in the required anchor size for the same system reliability.

1 **Introduction**

1.1 *The need for floating offshore wind (FOW)*

To meet net zero targets by 2050, decarbonisation of global energy supply will require a rapid expansion of offshore wind. The global offshore wind energy compact proposes a global ambition of 2000 GW by 2050 to meet the aims of the Paris Agreement (GWEC, 2022). Much of this growth will be provided by floating offshore wind (FOW) technology, which can be installed further from shore, where there is more available ocean space, high energy wind resources are located and conventional fixed offshore wind is not practical. Among the challenges of upscaling the production and installation of FOW systems is the need for efficient and reliable mooring and anchoring systems (Cerfontaine et al., 2023).

1.2 *Opportunities for more efficient mooring and anchor systems*

FOW infrastructure is subjected to a wide range of actions from metocean (e.g. wind and wave) and operational conditions, which are transmitted by mooring lines to the anchors that are typically embedded in the seabed. Taut mooring arrangements are attractive for FOW turbines as they require less length and lighter synthetic mooring line than traditional heavy chain catenary mooring arrangements. Taut moorings also transmit significantly higher mean and peak uplift tensions to the anchor compared to catenary moorings, where much of the mooring load is transmitted laterally and much of the load is taken by the weight of the chain. Further improvements to taut mooring configurations are currently being explored to reduce peak mooring uplift loads on the anchor through the development of load reduction devices (LRD) that achieve a non-linear stiffness profile with an initial compliant phase for operating conditions and a stiffer response at higher extensions to deal with extreme events (Gordelier et al., 2015; Dublin Offshore, 2021; Pillai et al., 2022; Lozon et al., 2022).

The seabed surrounding an embedded anchor also has potential to offer extra anchor capacity enhancements depending on the loads that are transmitted via the mooring lines to the anchoring system and surrounding seabed. For long-term cyclic loads that vary due to sea state and season during the whole-life or lifetime of the facility (e.g. 20 years), seabed strength, s_u, and therefore anchor capacity can evolve with time due to shearing and consolidation of the soil during sustained and variable low amplitude cyclic uplift loads (Blake et al., 2011; Cocjin et al., 2014; Smith & White, 2014; O'Loughlin et al., 2020; Zhou et al. 2020;; Gourvenec, 2020; Da Silva et al., 2021; Laham et al., 2021, Kwa et al., 2023a, c) . This can result in increases in the long-term embedded plate anchor capacity, Q_s, as defined below

$$Q_s = f(\{s_u\}) = N_c s_u A \quad (1)$$

where N_c is a bearing capacity factor (e.g. 13.11 for a rough circular plate anchor (Martin & Randolph 2001)) and A is the cross sectional area the anchor.

The strength $\{s_u\}$ can vary between the initial value, s_{u0}, the cyclically remoulded minimum s_{ur} and hardened maximum s_{uh} as a result of remolding and consolidation as defined in White et al. (2021). However, these long-term or whole-life increases in capacity are not typically considered in conventional geotechnical foundation capacity analysis. Under dynamic, high-amplitude loads, e.g. during a storm event, soil viscous rate effects can have a positive effect on the shear strength of the soil, depending on the strain rate as defined, for example, by eqn 2. (Randolph 2004).

$$s_u = s_{u0}\, max\left[1, 1 + \mu'\, sinh^{-1}\frac{\dot{\gamma}}{\dot{\gamma}_{ref}}\right] \quad (2)$$

where s_{u0} is the undrained soil shear strength defined at a slow or static strain rate as typically used in laboratory testing to evaluate s_u, μ' is a rate parameter, typically found to be ~0.1 (i.e. 10% extra strength per increment of strain), $\dot{\gamma}$ is a representative strain rate in the failing soil and $\dot{\gamma}_{ref}$ is a reference strain rate associated with the selected value of s_{u0}.

Wave-structure interaction can cause rapid, high amplitude snatch loads, which can have time periods ~10 times shorter than the wave itself (Hann et al., 2015). In this case extra dynamic anchor capacity is also created from mobilising the mass of the soil surrounding the plate (Kwa et al., 2021). This added soil mass can be described by the hydrodynamics 'added mass' term, which is well recognised in fluid mechanics and is routinely considered in the dynamic motion of floating structures and mooring lines, but is not considered in conventional geotechnical capacity analysis. The added mass for a geotechnical failure mechanism is typically double that for fluid flow around the same object (Kwa et al. 2021).

Allowing for this multiscale hierarchy of mooring-anchor-seabed load-time processes, which span from snatch loads (~10^0 s) to wave loading periods (~10^1 s), through to seabed consolidation durations (~$10^{4\text{-}6}$ s), over the full facility life (~10^{12} s) can have a beneficial design outcome, offering opportunities for reductions in anchor size and therefore, more efficient anchoring systems for FOW infrastructure. However, typical fluid-structure interaction models capture the response of floaters and mooring lines in the time-domain over relatively short time periods (i.e. up to 3 hours) rather than over a whole-life operational lifetime. They also model the connection of the mooring system to the seabed as a pin connection and so beneficial connected mooring-anchor-seabed interactions are not generally considered.

1.3 *Aim and outline of paper*

The aim of this study is to explore the benefits from connecting FOW mooring analyses of taut mooring line configurations with and without LRDs with anchor-seabed response. This is achieved through coupling a developing anchor macro model, *Ancmac*, with a Flexcom Finite Element Model (FEM) mooring-floater analysis of an International Energy Agency (IEA) 15 MW UMaine reference turbine in an idealised example design lifetime application.

2 Method: Anchor and floating system models

2.1 *Geotechnical anchor macro model*

Anchor macro models can be used to efficiently simulate the response of an anchor in terms of the resultant forces and displacements at the anchor, as an idealisation of the integrated effect of the surrounding elements of soil. This approach was formalised in the 1990s by Nova & Montrasio (1991), Houlsby et al., (1992) and Schotman (1989) by using a plasticity framework. The *Ancmac* model captures the anchor capacity as a time-varying function of the applied loads, reflecting short term processes of softening and pore pressure generation, u, and long-term processes of consolidation. Consolidation and pore pressure dissipation leads to hardening and strength gain over the anchor life time (Kwa et al., 2022, 2023c). A similar approach has also been implemented in an anchor macro model developed in Da silva (2021) and could be incorporated into other multi-directional anchor macro models (e.g. Yang et al. 2012; Cassidy et al., 2012).

The overall whole-life anchor simulation process is summarised in Figure 1 and is carried out using two software elements; *Ancmac* and a wrapper program, referred to as *K²M²*.

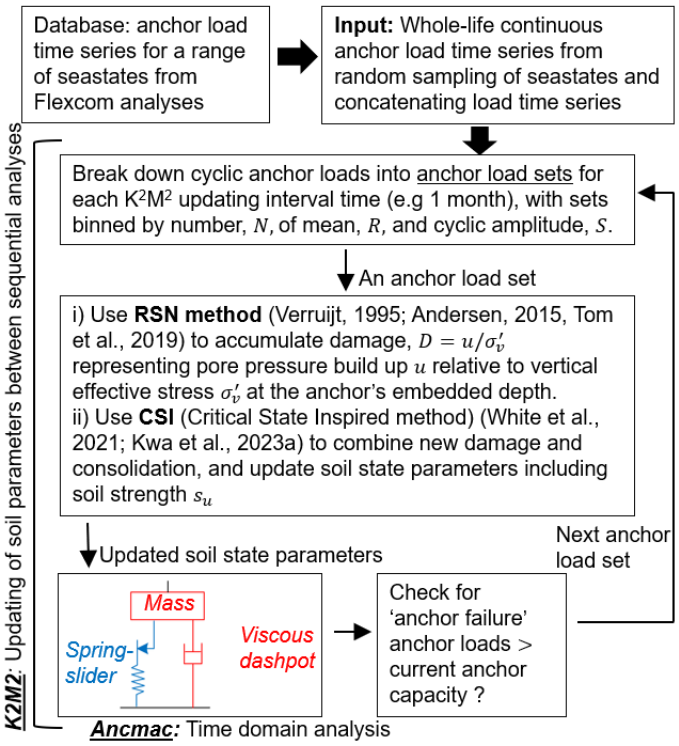

Figure 1: Flow chart of the anchor macro model routine

Ancmac represents the geotechnical anchor response using a one-dimensional parallel Iwan model (Iwan, 1967), in which the spring-sliders incorporate viscous rate effects, in combination with an added mass component. The detailed formulation of *Ancmac* and K^2M^2 can be found in Kwa et al., (2023a,b). The simulation routine of *Ancmac* when it is coupled with a separate numerical analysis package can be found in Kwa et al (2022).

2.2 *Hydrodynamic floating system model*

A hydrodynamic mooring-floater FEM in the commercially available software numerical analysis package Flexcom was used to model an International Energy Agency (IEA) 15 MW wind turbine and the Umaine Volturn-US semi-submersible FOW turbine. The full FOW turbine platform and turbine characteristics are described in detail in NREL publications (Evan et al, 2020; Allen et al., 2020). Flexcom FAST plug-ins AERODYN and SERVODYN were used to model the fully-coupled aero-hydro-servo response.

This modelling methodology has been validated against other software as part of an offshore code collaboration project OC6 (Robertson et al. 2020). Two taut mooring configurations were considered (a) a conventional taut mooring system, composed of high modulus synthetic polyester rope; (b) a taut mooring system, composed of the same polyester rope, with the addition of a polymer spring load reduction device (LRD) at each fairlead. This LRD is based on the Tfi Seaspring (Lozon et al., 2022) and can operate at high strain (20-50%), thus providing high levels of elongation to reduce dynamic loads on mooring lines and anchors. The LRD is modelled with a 3-phase nonlinear stiffness curve, to match the curve of the Tfi Seaspring The unstretched length of the LRD is modelled as 25 m, with a stretched length of 37.5 m at 4MN load. The general mooring parameters are shown in Table 1, with profile views of both mooring configurations shown in Figure 2.

Table 1: General mooring parameters of taut mooring system, applicable to both (a) conventional base case and (b) with LRD

Parameter	Value
Water depth, z_w	150 m
Number of mooring lines	3
Anchor radius from platform centerline	260 m
Seabed-mooring line angle, θ_m	34 deg
Polymer rope stiffness, $(EA)_{rope}$	7 MN
Polymer rope linear density ρ_{rope}	8.5 kg/m
Fairlead pre-tension, $T_{m,PT}$ *	2 MN

* with no applied wind or wave loads

Stochastic load cases were applied to the FOW turbine model based on the IEC design load case (DLC) matrix. From the matrix of load cases, two 'operational' load cases were selected, as well as two parked FOW turbine case for a storm and 1 in 50-year storm, as summarised in Table 2. All environmental loads are applied in the same direction, and each simulation was run for 10800s (3 hours). The resulting force time-series, T_m, was measured at the anchor point of the windward mooring line. The range (i.e. minimum, maximum and mean) values of T_m are summarised in Figure 3 for the taut conventional mooring and mooring with LRD cases. A typical comparison between the load-time series at the anchor point for the taut conventional mooring and mooring with LRD cases is summarised in Figure 4.

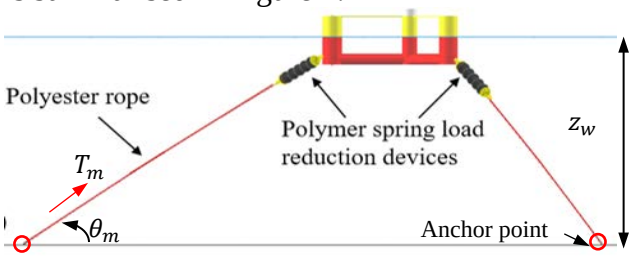

Figure 2: Profile view of taut mooring with load reduction devices (LRDs). The model of the conventional mooring system does not have the LRDs in the mooring lines.

Table 2: Summary of 3 load cases used in this study, selected from UMaine design matrix (Allen et al., 2020)

IEC DLC ref.	Load case description	Wind Speed (v_w) (m/s)	Sig. wave height (H_s)	Peak wave period (T_p)	Shape factor
1.1.4	Operational	4	1.1 m	8.52 s	1.00
1.1.12	Operational	12	1.84 m	7.44 s	1.00
6.3.38	Parked storm	38	6.98 m	11.70 s	2.75
6.1.47	Parked 1 in 50-yr storm	47.5	10.70 m	14.20 s	2.75

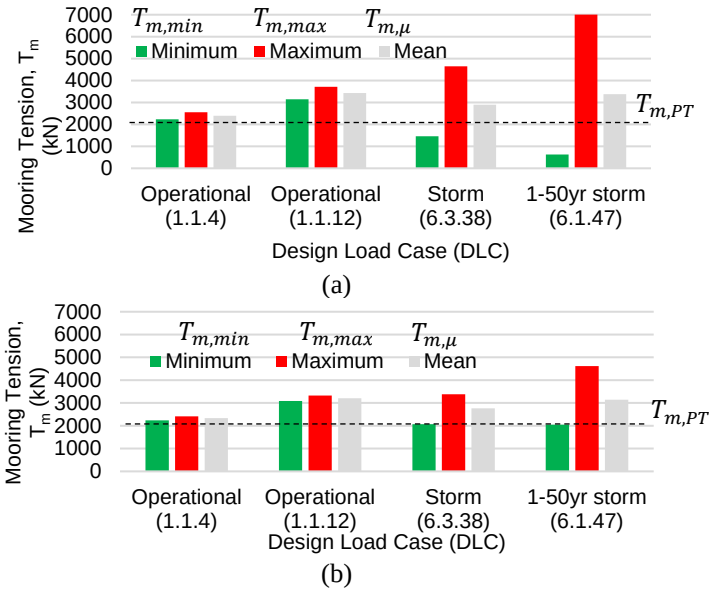

Figure 3: Summary of the range (minimum, maximum and mean) of loads at the anchor point for design load cases (DLCs as shown applied to (a) conventional taut mooring and (b) taut mooring with load reduction systems (LRD).

In both taut mooring cases, the mean loads, $T_{m,\mu}$ were higher than the pre-tensioned value, $T_{m,PT}$

($T_{m,\mu}$=2.3 to 3.4 MN), and there was an increasing variation between the minimum and maximum loads for the DLCs associated with higher windspeed. Including an LRD in the mooring configuration resulted in reduction in the maximum loads and load amplitudes transmitted to the anchor. This load reduction was particularly significant in the more severe storm loading cases; up to 37% reduction in the parked regular storm case and 50% in the 1-in-50-year storm case. Smaller reductions of 5 to 11% were observed in the operational cases as a result of including LRDs in the mooring configuration.

These load-time-series were used to build synthetic yearly realisations reflecting seasonality in anchor loads in the example whole-life application as described and discussed in Section 3.

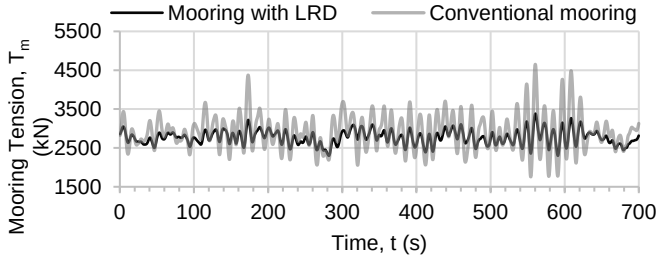

Figure 4: Example comparison between loads transmitted to the anchor for taut mooring configurations with and without LRD (for DLC 6.3.38)

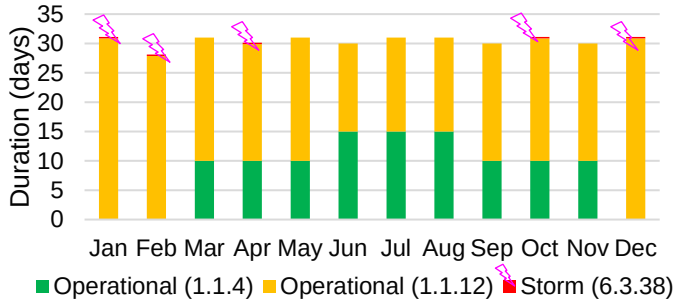

Figure 5: Selected seasonal variations in metocean conditions.

2.3 *Applied whole-life metocean conditions and initial seabed conditions*

To build the synthetic seasonally-varying yearly realisations of whole-life anchor loads, illustrative combinations of the DLCs were chosen to artificially reflect seasonally-varying metocean conditions within a year (i.e. calmer in summer and more severe in winter) as shown in Figure 5. This combination of DLCs was repeated over 20-years to idealise a design lifetime of a FOW turbine. To investigate the response of the system under an extreme loading event, a 1 in-50-year storm was additionally applied for a period of 3 hours in the 15th year of the design lifetime.

It is assumed that these loads are transmitted directly to the anchor, whereas in reality, additional geotechnical resistance would be mobilised from interactions between the embedded section of mooring line and the seabed. Based on analytical solutions for the frictional capacity of embedded anchor chains (Neubecker & Randolph 1995), this decrease in load would be less than ~10% and is neglected in this analysis.

An illustrative set of seabed input parameters to *Ancmac* and *K^{2}M^2* were selected to be representative of lightly over consolidated clay around a circular plate anchor embedded at a depth of ~20m. The selected seabed values were an initial undrained strength s_{u0}=80kPa, coefficient of consolidation base case value of c_v=6m^2/s and a variation case of 12m^2/s, and a sensitivity S_t=2.5 at the anchor point. These selected seabed values were similar to those in centrifuge tests performed by O'Loughlin et al., (2020) and Zhou et al., (2020).

Two sets of simulations were also considered; one where seabed strengthening or hardening was disabled and another set where seabed hardening was enabled. When seabed hardening was disabled, seabed strength, s_u, is limited to vary between the initial value, s_{u0}, and a cyclically remoulded minimum, s_{ur}. When seabed hardening is enabled, both seabed softening and beneficial whole-life seabed strengthening effects from consolidation were considered in the analysis, and as a result, s_u is allowed to vary between s_{ur} and hardened maximum s_{uh} from consolidation. This change in s_u affects the through-life available anchor capacity Q_s according to Equation 1, which is compared with T_m to find the required anchor sizes.

3 Results and discussion: An integrated whole-life geotechnical-hydrodynamic application

3.1 *Basis for defining required anchor size*

Results are presented for the 15MW taut-moored FOW turbine, with and without an LRD in the mooring line, with a deeply-embedded circular plate anchor. Anchor capacity is updated on a monthly basis, so a monthly factor of safety (FoS) is calculated based on eqn 3.

$$FoS = Q_s/T_{m,max} \quad (3)$$

To determine the required anchor size for each case, a minimum factor of safety, FoS ≥1 is set over the 20-year design lifetime in the simulations. The analysis of the anchor response throughout the design lifetime was repeated, iterating the anchor size each time, to find the minimum anchor size that meets this condition. For deeply-embedded circular plate anchors, the capacity is proportional to the cross sectional anchor area.

This adopted criteria of FoS ≥1 is a lower FoS than could be accepted according to conventional design practice, but is used here to provide a simple consistent basis to compare different modelling cases (with and without LRD, with and without seabed hardening). A change in the required FoS would not affect the relative performance for different cases, only the absolute results (i.e. the required anchor

size). The minimum required anchor sizes for each of the four simulation cases are summarised in Figure 6.

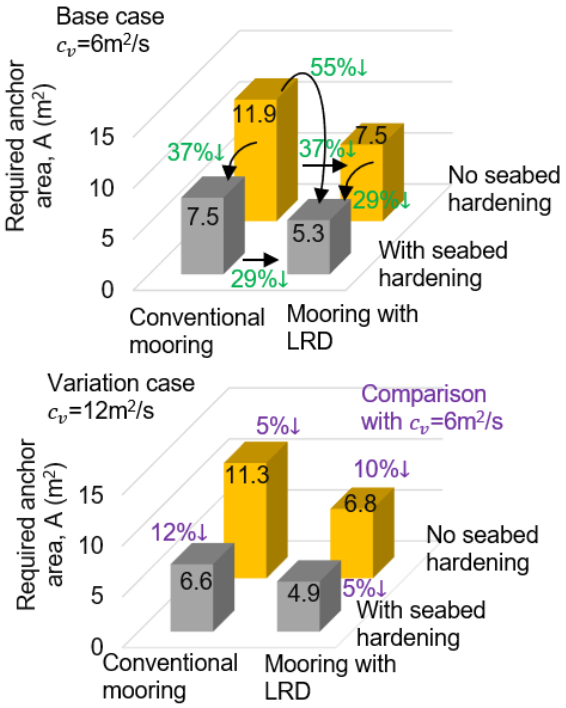

Figure 6: Comparison of required anchor sizes for FoS ≥ 1

The differences in required anchor size are created by two effects. Firstly, the use of a LRD in the mooring line reduces the loading at the anchor. Secondly, the anchor capacity varies through the design life depending on (i) the applied loading, (ii) whether seabed hardening is modelled and (iii) the consolidation coefficient of the seabed, which controls the rate of strength regain. These effects are illustrated by the time evolution of the key loading (Q_s and $T_{m.max}$) and soil parameters (s_u, H and D), which are shown in Figure 7 and 9 for the conventional mooring case and the mooring with LRD case. The resulting variation in FoS over the design life for each case is shown in Figure 8 and 10.

3.2 *Results for conventional mooring*

In the conventional mooring case, $T_{m,max}$ varied between 3.7 to 4.6 MN as a result of the selected yearly metocean conditions (Figure 5). As a result of these loads, the anchor capacities reduced significantly to a minimum value of approximately 0.6× the initial anchor capacity Q_{s0} and undrained seabed strength, s_{u0} within the first year of the simulated design lifetime as shown in Figure 7a and b. This initial drop in anchor capacity also corresponded to a decrease in the through-life FoS as shown in Figure 8.

This initial drop in anchor capacity during the first year, was a result of the seabed softening under cyclic loading and because insufficient time has passed to allow consolidation and dissipation of damage or pore pressure generated by the applied anchor loads.

For the no-hardening case, this seabed softening response dominated and the available anchor capacity remained at $0.6 \times s_{u0}$ and Q_{s0} (as shown by the dotted lines in Figure 7. Consequently, the anchor size is set by the requirement to resist the higher applied anchor loads from the 1 in 50-year storm in year 15 to achieve a FoS ≥ 1, as marked by F' in Figure 7a and 8b.

If hardening was enabled in the simulations, the required anchor size is instead controlled by the initial drop in anchor capacity and the requirement for FoS ≥ 1 (marked as F in Figure 7a and 8a) during the initial year. After year 1, seabed strengthening eclipsed the effect of damage from the applied loads resulting in an increase in capacity towards $1.3\times s_{u0}$ and Q_{s0}, as shown by the solid lines in Figure 7a to c. This increase in available anchor capacity resulted in FoS >1 when the 1 in 50-year storm was applied at year 15 and corresponded to 37% decrease in the required anchor size (i.e. 7.5 vs. 11.9 m^2) as shown in Figure 5.

3.3 *Results for mooring with LRD*

When LRDs were present in the mooring lines, smaller anchor loads were applied. $T_{m,max}$ varied between 3.3 to 3.4 MN and reached a peak of 4.6 MN during the 1 in 50 year storm as summarised in Figure 4. Compared to the no-LRD case, this resulted in less seabed damage, D, as well as smaller and more gradual increases in hardening, H, undrained strength, s_u, and anchor capacity, Q_s, as shown in Figure 9. The final values of seabed strength, s_u, and anchor capacity, Q_s, were similar in the cases with or without LRDs. Therefore, with soil hardening, it is possible to have a 29% decrease in the required anchor size (i.e. 5.3 vs 7.5 m^2) if LRDs are present in the mooring configuration compared to the no-LRD case.

When seabed hardening was enabled the required anchor sizes were determined based on the initial drop in anchor capacity, Q_s and FoS in the first year, FoS≤1 (marked as F in Figure 9a and 10a), the same as for the no-LRD case. This is because the seabed strengthened and hardened in subsequent years such that FoS >1 when the 1 in 50 year storm was applied in year 15.

When hardening was not enabled, the anchor size depended on the anchor capacity when the 1 in 50 year storm was applied in year 15 (marked as F' in Figure 9a and 10b). This anchor size was larger than when hardening was enabled (7.5 vs 5.3 m^2).

When both LRD and whole-life seabed effects are considered together, the required anchor size is reduced by 55% compared to the case where conventional mooring is used and no seabed hardening is considered (i.e. 5.3 vs 11.9m^2), as shown in Figure 6.

3.4 *Variation: higher consolidation coefficient, c_v*

Increasing the coefficient of consolidation from c_v=6 to 12 m^2/s increases the rate of seabed hardening H, and recovery of applied damage, D, as shown by the green and blue lines in Figure 7 and 9.This increase in c_v resulted in a 5 to 12% decrease in anchor size for all cases as shown in Figure 6.

3.5 *Full coupling of anchor and mooring response*

This analysis uses a FoS limit on the static anchor capacity to define the required anchor size. It does not consider movement of the anchor, and the loads come from a mooring analysis in which the anchor is represented as a fixed pin. Further design efficiencies could result from considering anchor ductility, where the anchor can move beyond its installed position and also mobilise seabed added mass. This is explored in more detail in Kwa et al. (2022; 2023d).

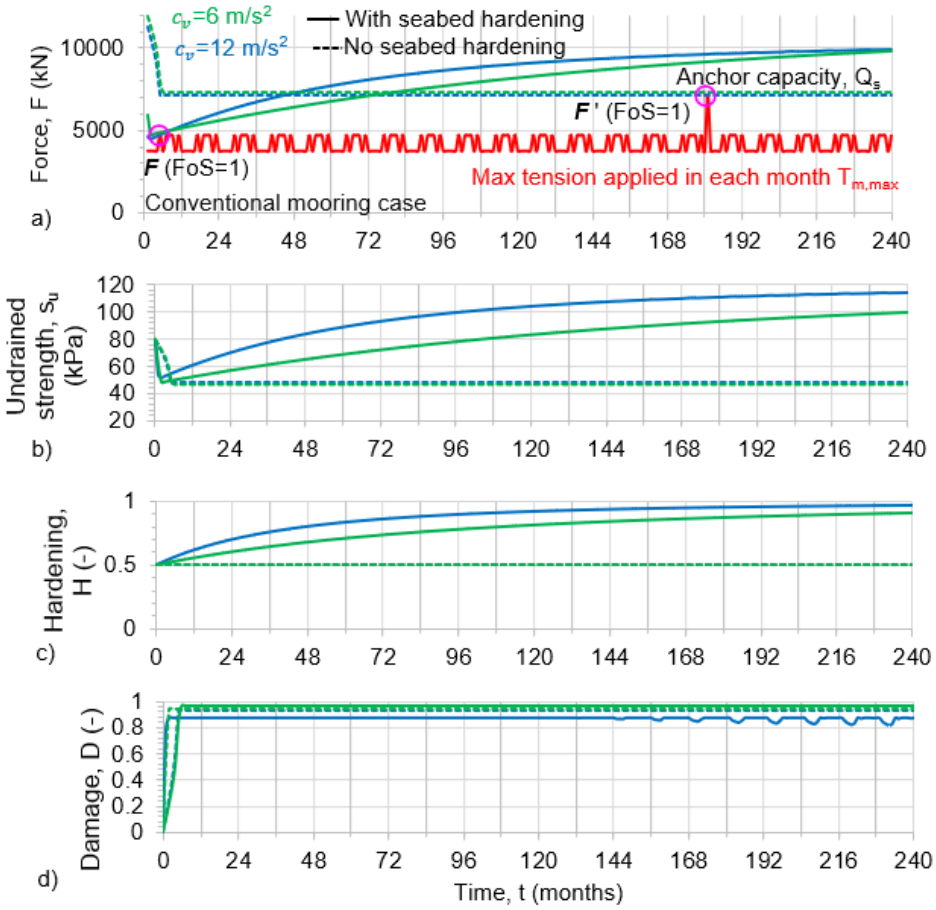

Figure 7: Summary of (a) anchor capacity relative to applied tension loads (b) changes in seabed undrained strength, (c) hardening and (d) damage for conventional taut mooring case

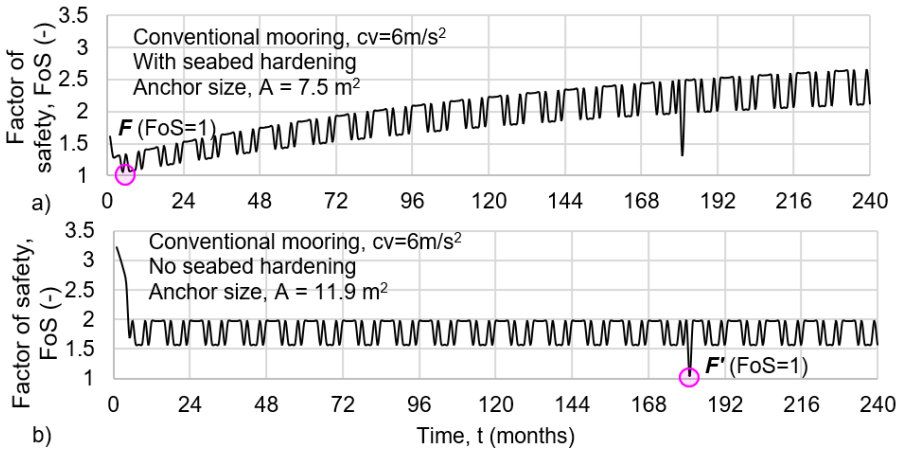

Figure 8: Changes in through-life factor of safety (FoS) (a) with seabed hardening and (b) without seabed hardening for the conventional taut mooring case

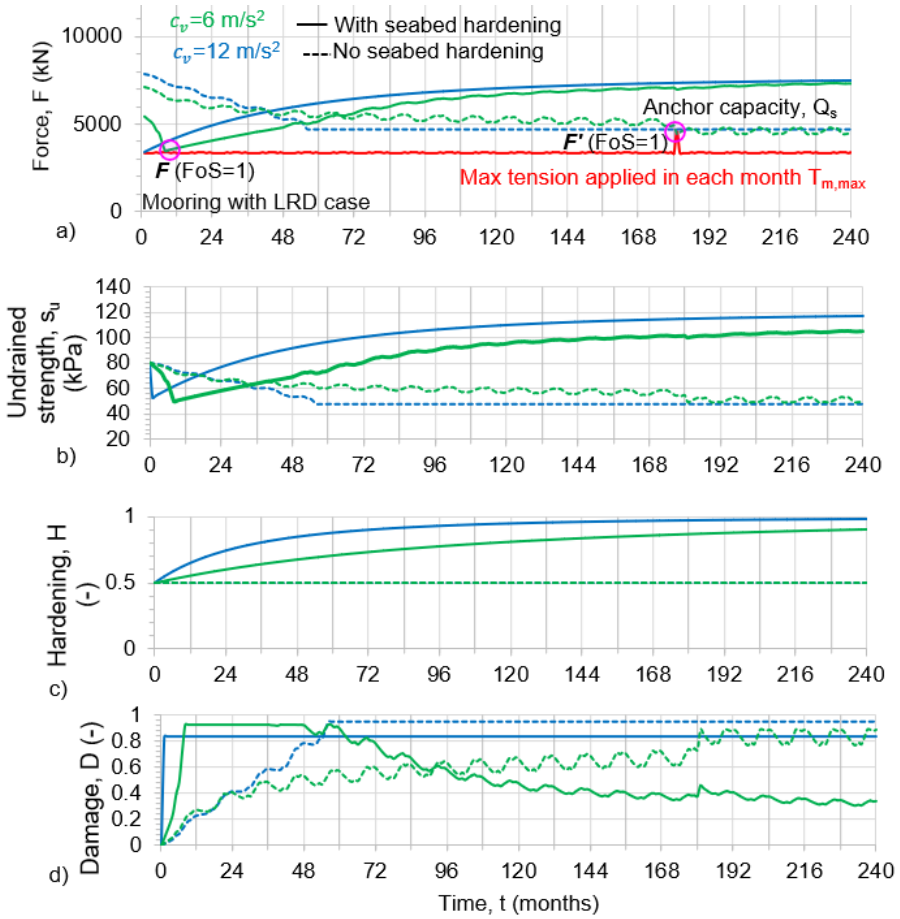

Figure 9: Summary of (a) anchor capacity relative to applied tension loads (b) changes in seabed undrained strength, (c) hardening and (d) damage for mooring with LRD case

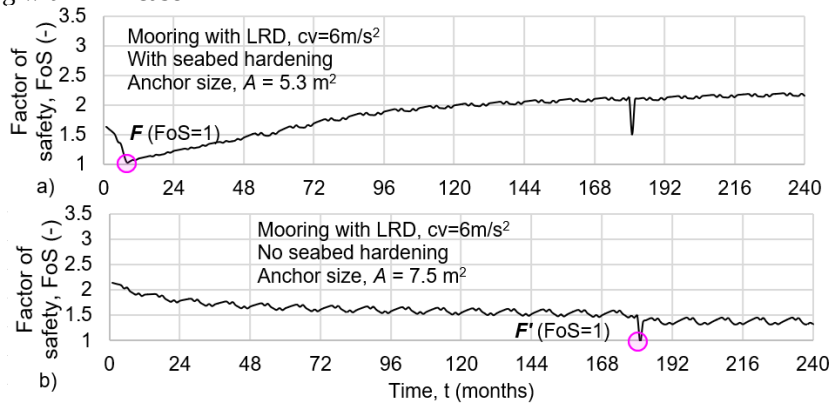

Figure 10: Changes in through-life factor of safety (FoS) (a) with seabed hardening and (b) without seabed hardening for the taut mooring with LRD case

4 Conclusions

Coupling floater-mooring analyses with whole-life anchor-seabed response uncovers opportunities for more efficient mooring and anchoring systems for floating offshore wind. Results from an example whole-life analysis show that if load reduction devices (LRDs) are included in the mooring configuration when deriving anchor loads, this can result in a 29 to 37% decrease in required anchor size. If beneficial whole-life anchor-seabed effects are considered separately, this can result in a similar decrease in anchor size. If both factors (LRDs and whole-life seabed are considered together, it is possible to approximately halve the required anchor size. The coupling between the floater-mooring and whole-life anchor-seabed response can be achieved efficiently via a developing anchor macro model, *Ancmac* that simply and practically connects with floater-mooring analyses, to assess through-life changes in anchor capacity and seabed response during the full operational lifetime of FOW infrastructure.

5 Acknowledgements

This work forms part of research supported by the Royal Academy of Engineering under the Research Fellowship Programme, RAEng Chair in Emerging Technologes Centre of Excellence in Intelligent & Resilient Ocean Engineering (IROE), and Supergen ORE Hub (Grant EPSRC EP/S000747/1). Katherine

Kwa is supported by the RAEng Research Fellowship Scheme, David White is supported by the Supergen ORE Hub, Susan Gourvenec is supported by the Royal Academy of Engineering through the Chair in Emerging Technologies scheme, and Adam Sobey is supported by The Lloyd‘s Register Foundation.

6 References

Allen, C. et al. (2020) Definition of the UMaine VolturnUS-S Reference Platform Developed for the IEA Wind 15MW Offshore Reference Wind Turbine. NREL/TP-5000-76773

Andersen, K.H. (2015). Cyclic soil parameters for offshore foundation design. Front. in offshore geotech. III 5-82.

Bransby, M.F. (2002) The undrained inclined load capacity of shallow foundations after consolidation under vertical loads. Num models in geom. NUMOG VIII, 431-437

Blake et al., (2011) Setup following keying of plate anchors assessed through centrifuge tests in kaolin clay. In Proc. ISFOG 2011, Perth, Australia (pp. 8-10).

Cassidy M.J. et al. (2012). A plasticity model to assess the keying of plate anchors. Géot., 62(9): 825–836

Cerfontaine, B., et al. (2023) Anchor geotechnics for floating offshore wind: current technologies and future innovations, J. Ocean Eng. 279, p. 114327

Cocjin M., et al. (2014). Tolerably mobile subsea foundations – Observations of performance. Géot. 64(11): 895-909.

Crown Estate (2020. Broad horizons: Key resource areas for offshore wind. Summary report

Deeks, A., et al. (2014) Design of direct on-seabed sliding foundations, OMAE2014-24393, V003T10A024

DNV (2002). DNG-RP-E02: Recommended practices: design and installation of plate anchors in clay. DNV

Dublin Offshore (2021) Executive Summary-Load Reduction Device, Dublin Offshore.

Evan, G. et al. 2020. Definition of the IEA 15-Megawatt Offshore Reference Wind. Golden, CO: National Renewable Energy Laboratory. NREL/TP-5000-75698.

Gordelier, T et al. (2015). A novel mooring tether for highly-dynamic offshore applications; mitigating peak and fatigue loads via selectable axial stiffness. J. of Marine Sc. and Eng., 3(4), pp.1287-1310.

Gourvenec S. (2020) Whole-life geotechnical design: What is it? What’s it for? So what? & what next? Proc. 4th ISFOG. 2021, Austin, Texas, USA, ASCE Geo-Institute & DFI

Hann, M., et al. (2015). Snatch loading of a single taut moored floating wave energy converter due to focussed wave groups. J. Ocean Eng., 96, pp.258-271.

Houlsby, G. T., & Wroth, C. P. (1991). The variation of shear modulus of a clay with pressure and overconsolidation ratio. Soils & Found., 31(3), 138-143.

Iwan, W. D. (1967). On a class of models for the yielding behavior of continuous & composite systems.

Kwa, K.A., et al. (2021a). Analysis of the added mass term in soil bearing capacity problems, Geot. Let. 11, pp. 80-87

Kwa, K.A. et al. (2022) A numerical macro model to simulate the whole life response of anchors for floating offshore renewable energy systems. OMAE 2022-81101

Kwa, K.A., et al. (2023a) The RSN-CSI model: A whole life geotechnical anchor macro model for floating offshore systems (under review)

Kwa, K.A., et al. (2023b) A whole-life macro model of anchor capacity for floating offshore renewable energy systems, NUMGE, London, UK

Kwa, K. A., & White, D. J. (2023c). Numerical modelling of plate anchors under sustained load: the enhancement of capacity from consolidation. Comp. & Geot., 158, 105367.

Kwa et al., (2023d) Dynamic seabed-anchor capacity enhancements for taut-moored floating offshore wind. SEG 2023, Delft (Extended abstract under review)

Laham, N. I., et al. (2021). Episodic simple shear tests to measure strength changes for whole-life geotechnical design. Géot. Let., 11, 103-111.

Lozon. E et al. (2022). Design and Analysis of a Floating-Wind Shallow-Water Mooring System Featuring Polymer Springs: Golden, CO: NREL/CP-5000- 83342.

Martin, C. M. & Randolph, M. F. (2001). Applications of the lower and upper bound theorems of plasticity to collapse of circular foundations. In Proc. 10th Int. Conf. on Computer Methods and Advances in Geomechanics,

Neubecker, S.R. & Randolph, M.F., 1995. Profile and frictional capacity of embedded anchor chains. Journal of geotechnical engineering, 121(11), pp.797-803.

Nova R. & Montrasio L (1991) Settlements of shallow foundations on sand. Geot.,41(2): 243-256.

Pillai AC, et al. (2022) Anchor loads for shallow water mooring of a 15 MW floating wind turbine — Part I: Chain catenary moorings for single and shared anchor scenarios, Ocean Engineering, vol 266, 111816.

O'Loughlin, C. D., et al. (2020). Load-controlled cyclic T-bar tests: a new method to assess effects of cyclic loading & consolidation Géot. Let., 10(1), 7-15.

Da Silva, A.P. et al. (2021a). A non-associative macro-element model for vertical plate anchors in clay. Can. Geo. J 58(11), p.1703-1715

Da Silva, A.P. et al., (2021b). A cyclic macro-element framework for consolidation dependent three dimensional capacity of plate anchors, J. Mar. Sc & Eng. ((2), 199

Da Silva, A. P. (2021c). Macro-element modelling of plate anchors for floating offshore structures accounting for capacity changes during operational conditions PhD Thesis.

Randolph, M., (2004). Characterisation of soft sediments for offshore applications, In Proc. Geot.& Geophys. Site Charac., Portugal, p.209-232

Robertson, A. N., et al. (2020). OC6 Phase I: Investigating the underprediction of low-frequency hydrodynamic loads and responses of a floating wind turbine. In J. of Physics: Conference Series (Vol. 1618, No. 3, p. 032033).

Schotman, G.J.M. (1989). The effects of displacements on the stability of jackup spudcan foundations'. Proc. 21st Offshore Tech. Conf., Houston, Texas, OTC 6026.

Smith V. B. & White D. J. (2014) Volumetric hardening in axial pipe soil interaction. In Proc. Offshore Tech. Conf. Asia, OTC ASIA 2014 (Vol. 2, pp. 1611-1621).

Stanier, S.A. & White, D.J., (2018). Enhancement of bearing capacity from consolidation: due to changing strength or failure mechanism?. Géot, 69(2), pp.166-173.

Tom, J.G., et al., 2019, June. Fluid-structure-soil interaction of a moored wave energy device. In International Conference on OMAE (Vol. 58899, p. V010T09A024). ASME

Verruijt, A. (1995). Computational geomechanics (Vol. 7). Springer Science & Business Media.

White, D. J., et al. (2021). A cyclic py model for the whole-life response of piles in soft clay. Comp. & Geot., 141, 104519.

Yang, M. et al., (2012). Behaviour of suction embedded plate anchors during keying process. J. Geot. & Geoenv. Eng. 138(2), pp.174-183.

Zhou, Z., et al. (2020). Improvements in plate anchor capacity due to cyclic and maintained loads combined with consolidation. Géotechnique, 70(8), pp. 732-749.